신경회로망을 이용한 SRM 센서리스 제어연구

論 文
50B-1-5

Sensorless Control of SRM Using Neural Network

崔 載 東* · 安 載 晃** · 成 世 鎭***
(Jae-Dong Choi · Jae-Hwang An · Se-Jin Seong)

Abstract - This paper introduces a new indirect rotor position estimation algorithm for the SRM sensorless control, based on the magnetizing curves of aligned and unaligned rotor positions. Through the basic test method, the complete SRM magnetizing characterization is first constructed using a neural network training, and then used to estimate the rotor position. And also, the optimal phase is selected by the phase selector. In order to verify this approach, the proposed rotor position estimation algorithm using a neural network learning data is investigated. The experimental results show that the proposed control algorithm can be effectively applied to SRM sensorless control.

Key Words : Switched Reluctance Motor, Sensorless speed control

I. Introduction

Switched Reluctance Motor(SRM) is gaining much attention due to its simplicity and low cost. Its simple construction make the SRM drive an interesting alternative to compete with permanent magnet brushless DC motor and induction motor drives. The conduction angle can be chosen through the precise rotor position sensors due to the high system efficiency over a wide range of speed. Usually, an encoder, resolver or Hall sensor attached to the shaft is used to supply the rotor position. However the use of these expensive sensors may has less fault-tolerant capability than motor in harsh environment. Therefore, it may lead to reliability problems and the limitation of motor drive application range. Recently, there has been much interest in techniques for eliminating of the direct rotor position sensors, and it has been simplified by indirect determination of the rotor position. The chopping current detection technique[1], flux-current detection technique [2][3], impedance sensing[1][4], modulation technique[4], current gradient sensorless method[7][8], and estimation of immediate rotor position using current modification technique[8] has been proposed to detect the indirect rotor position. Most of the original principle is based on magnetizing characteristics of SRM. These indirect rotor sensing methods have advantages such as elimination of sensors, decreasing size, no effect at external element, increasing reliability and a wide speed range. Therefore the exact information of rotor position using the indirect method is required to the good performance of SRM drive.

Mechanical sensor is expensive and unreliable in industrial and automotive environment, therefore the so-called sensorless control techniques are attractive. This paper proposes the indirect rotor position estimation algorithm having the high precision for SRM drive. The flux linkage is calculated from the measured phase voltage and phase current, and the calculated data are used as the input of magnetizing profiles for rotor position detection. Each of the magnetizing profiles consisted of the method using the neural network which applies to the non-linear characteristics analysis and the method to select optimal angle is proposed for the rotor position detection. The rotor position detection method using neural network is executed the off-line considering time delay due to learning time. The tolerance analysis results of proposed method and the indirect rotor position estimation algorithm are verified by comparing with the measured results from the direct rotor position sensor over a wide range of speed.

2 Flux Linkage Model

As shown at figure 1, the system for the typical SRM

* 正 會 員 : 韓國航空宇宙硏究院 先任硏究員 · 工博
** 正 會 員 : 忠南大 工大 電氣工學科 博士課程修了
*** 正 會 員 : 忠南大 工大 情報通信工學部 敎授 · 工博
接受日字 : 2000年 8月 4日
最終完了 : 2000年 12月 26日

drive with PI controller consists of a chopper, inverter, voltage and current detection circuit including filter and DSP control board. The chopper is used for variable voltage source with the constant current. The feedback signals required at control loop are sensed from the phase voltage and phase current. At first, the sensed signals are filtered via analog filter within the voltage and current sensing circuit. And it had filtering through the internal digital filter of processor again.

The SRM can be modeled by its torque equation and described as electromechanical machine.

$$T_e = \frac{1}{2}[i]\frac{d[L]}{d\theta}[i]^T \tag{1}$$

where $[i]=[i_a, i_b, i_c]$, $[\lambda]=[\lambda_a, \lambda_b, \lambda_c]$ and

$$[L]=\begin{bmatrix} L_{aa} & L_{ab} & L_{ac} \\ L_{ba} & L_{bb} & L_{bc} \\ L_{ca} & L_{cb} & L_{cc} \end{bmatrix}$$

in the case of 6/4 SRM. Inspecting Equation (1), we are convinced that taking flux linkage as the state variables is a better approach of SRM modeling than the winding inductance because the number of variables are reduced dramatically, from 16 to 4 in the case of 8/6 motor as well as from 9 to 3 for 6/4 motor.

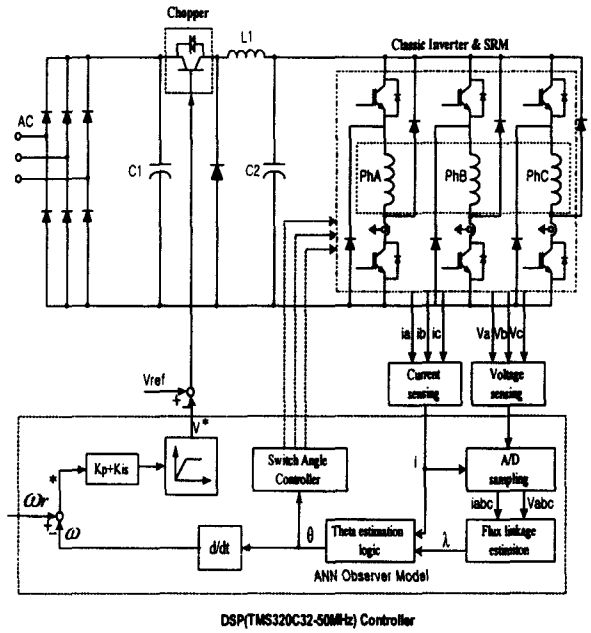

Fig. 1 Block diagram of the proposed SRM sensorless PI control system using ANN observer model.

As the SRM Modeling in terms of winding inductance needs a number of winding inductances with high nonlinearity, requires mutual inductance, computation and measurement for flux linkage are more direct and simpler than that for inductance. The basic methods to obtain the detailed SRM magnetizing characteristics are finite element analysis and experimental testing method. The phase voltage equation of a non-linear series R-L circuit excited by dc power supply is used to get SRM magnetizing characteristics. The phase voltage equation is given by

$$V = Ri + \frac{d\lambda}{dt} \tag{2}$$

Where V is the applied voltage, λ is flux linkage and R is the winding resistance. The flux linkage can be computed as

$$\lambda = \int_0^i (V - Ri)dt \tag{3}$$

Where i is the steady state current.

The transient state of current(i) and voltage(v) is recorded at microprocessor and the data are computed to obtain the flux linkage by Equation(3). As the SRM modeling in terms of the voltage-current(v-i) measurement circuit of Figure 1 are measured from unaligned position to aligned position at each $\Delta\theta = 2^\circ$. The flux linkage-current($\lambda - i$) characteristics to determinate inductances are obtained by the experiment.

The experimental data of v-i profile for the particular rotor position are used to obtain flux(λ) as the current (i) function by $\lambda = f(i)$. The differential of this function gives the inductance value for required current and rotor position. Figure 3 shows the measured flux-current profile and inductance profile.

In the case of SRM, the sensorless techniques can use the reluctance variation itself to detect the rotor position. By using this approach it is possible to obtain rotor position information from the electrical terminal quantities of machine. To this aim the flux linkage can be estimated via calculation of the phase voltage and current. Usual approaches present limitations for accuracy and are computationally intensive.

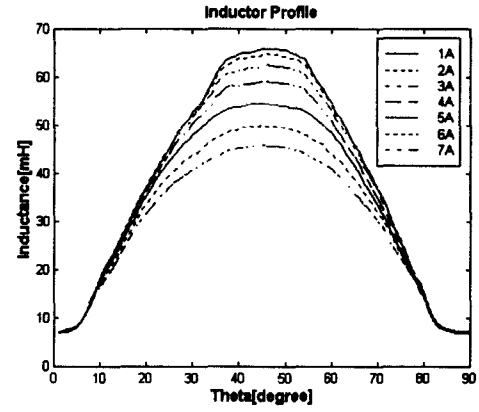

Fig. 2 Measured inductance profile

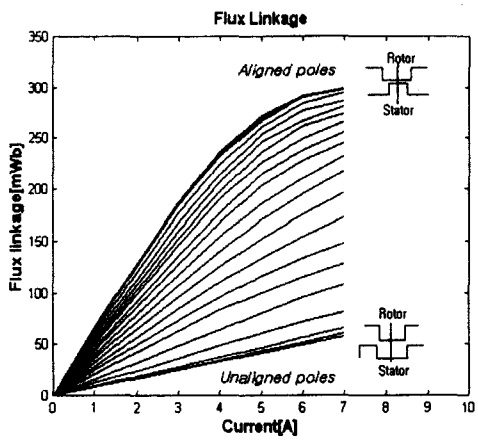

Fig. 3 Measured flux-current profile

Therefore, a simple solution using neural network is proposed for mapping the rotor position from the flux and current in this section.

3. Rotor Position Estimation Algorithm

The purpose of SRM magnetizing characteristic modeling using neural network is to obtain the estimated variables based on SRM with the non-linear characteristic. And it also need to get the exact solution through the learning of the analysis results for each of current when the rotor position changes.

For the SRM application, the training data set is comprised of the flux linkage(λ) and current(i) as inputs and the corresponding position(θ) as output. By given a sufficiently large training data set, the Artificial Neural Network(ANN) can build up a correlation among flux linkage(λ), current (i) and rotor position(θ) for an appropriate network architecture. Then this off-line trained ANN can be evaluated against a test data set which has different λ -i values. Figure 4 shows how the ANN is trained off-line. Figure 5 and 6 show the input data and training result of ANN, respectively.

The result of training by ANN is used to model the flux observer. A large amount of computation time is required to consist of position estimation of real time learning method in terms of on-line composition.

Therefore, in this paper, the rotor position predictor consists of obtained lookup table from the on-line ANN training. Figure 7 shows the block diagram of it.

In the figure 7, the initial flux linkage calculates to obtain the initial predicted position θ_p from phase voltages and currents. And the position correction corrects continuously the initial predicted position θ_p in order to obtain the final estimated position θ_e. Then the

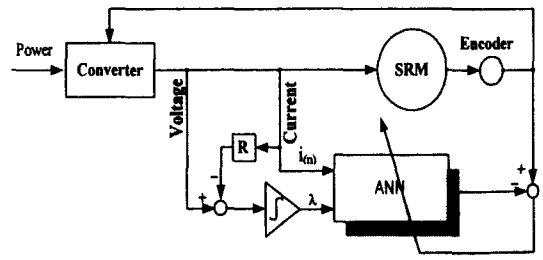

Fig. 4 An ANN off-line training method

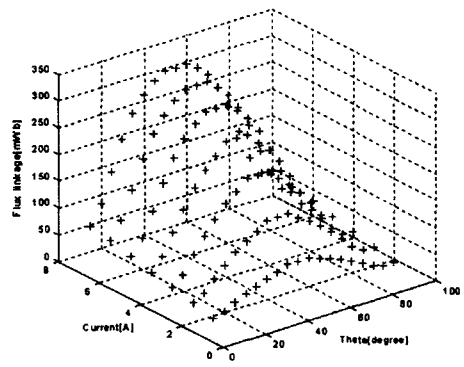

Fig. 5 Input data for ANN training from the measured results

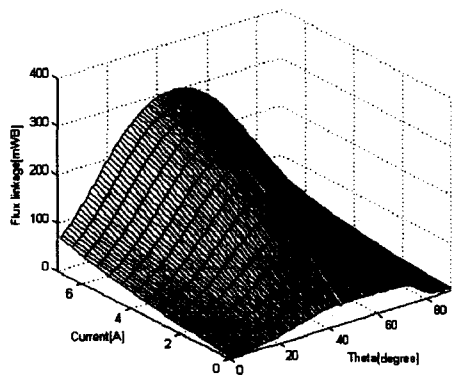

Fig. 6 Magnetizing Curves from ANN Training

flux linkage, current and position in each phase can be expressed as

$$\lambda = \lambda(i,\theta) \tag{4}$$

$$i = i(\lambda,\theta) \tag{5}$$

$$\theta = \theta(i,\lambda) \tag{6}$$

Therefore, a small perturbation in λ, i and θ can be expressed as follows

$$\Delta\lambda = \left[\frac{\partial\lambda}{\partial i}\right]_{\theta=const} \cdot \Delta i + \left[\frac{\partial\lambda}{\partial\theta}\right]_{i=const} \cdot \Delta\theta \tag{7}$$

$$\lambda_e = \lambda + \Delta\lambda \tag{8}$$

$$\Delta\theta = \left[\frac{\partial\theta}{\partial i}\right]_{\lambda=const} \cdot \Delta i + \left[\frac{\partial\theta}{\partial\lambda}\right]_{i=const} \cdot \Delta\lambda \tag{9}$$

$$\theta_e = \theta_p + \Delta\theta \tag{10}$$

Where λ_e is the estimated flux linkage, θ_e is extrapolated linearly by using previous and actual position values. The flux linkage for each phase can be predicted by Equation (3). In real implementation, the current is more likely to have less errors than the flux linkage which is predicted by the integration of the phase voltage.

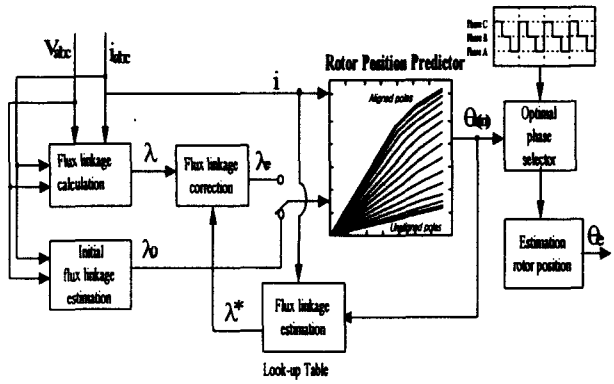

Fig. 7 Angle measurement algorithm by the flux-current method

Therefore, the model that assumes $\Delta i = 0$ has the smallest error. If we assume that current ($\Delta i = 0$) has no error at Equation(7), Equation (11) can be obtained from the condition of $\Delta i = 0$

$$\Delta\theta = \left[\frac{\partial\theta}{\partial\lambda}\right]_{i=const} \cdot \Delta\lambda \tag{11}$$

Depend on the required accuracy, the angle correction itself is repeated for several times. At the next level, θ_p is corrected to make $\Delta\theta$ after comparing the flux linkage $\lambda_e = (\theta_p, i)$ measured with the real flux linkage (λ) to become $\Delta\lambda$. To determinate the final angle value $\theta_{e(n)}$, each estimated phase angle is multiplied by its respective confidence value found from the optimal phase selector, and the total is divided by the addition of all the confidence factors.

$$\theta_e = \frac{\theta_1 \cdot C_A + \theta_2 \cdot C_B + \theta_3 \cdot C_C}{C_A + C_B + C_C} \tag{12}$$

Where θ_e is the final angle estimate, θ_1, θ_2 and θ_3 are the phase angle estimates of phase A, B and C, respectively. C_A, C_B and C_C are the confidence values of each phase. The position estimation is less accurate in the region closed to unaligned and aligned position due to the small changes in $[\partial\lambda/\partial\theta]_{i=const}$. Therefore, to estimate the position from the best phase among all conducting phases, we chose the optimal region (8° ~38°) where $[\partial\lambda/\partial\theta]_{i=const}$ is the maximum at each phase and used as the optimal position estimator as shown Figure 8.

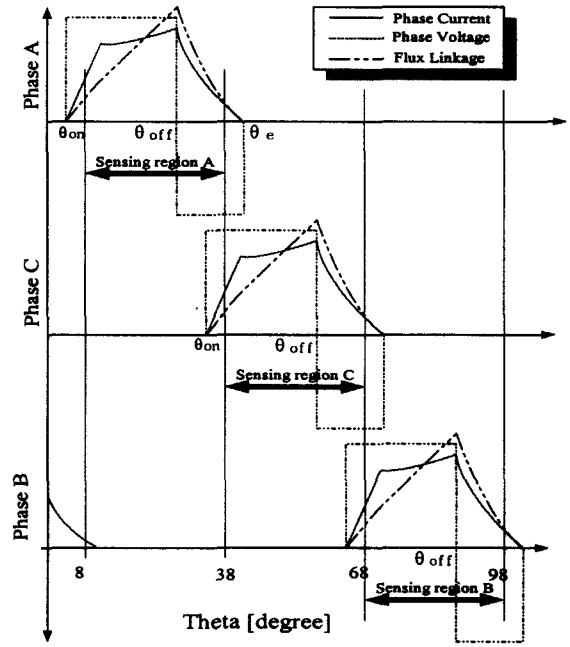

Fig. 8 Optimal sensing region according to rotor Angle

4. Experimental Results

The experimental results of angle measurement algorithm using the neural network are presented in this paper. The experimental results are implemented for the single pulse mode of motor with a steady state speed at 1000 rpm and 1500 rpm. Therefore, in the single pulse mode, the current waveform is regular and the flux has a simple profile, quasi-triangle wave-shape when the motor reaches at a steady state with 1000 rpm and 1500 rpm. Table 1 shows the design parameters of motor used to the experiment.

The lookup table of rotor position algorithm using the measured data was constructed at section II. The unaligned and aligned position are 0° and 45° respectively.

We chose the region where $[\partial\lambda/\partial\theta]_{i=const}$ is the maximum at each phase and used as the optimal position estimator. Then phase A, B and C are chosen in order and the optimal position information is given. The estimated angle errors have the maximum ± 1° at 1000

rpm and the maximum ± 1.5° at 1500 rpm due to the sampling frequency 10kHz. As it closes to the aligned position, the value of $[\partial\lambda/\partial\theta]_{i=const}$ becomes small, thus the errors become more high.

The figure 9 and figure 10 show the real angles measured from encoder and the estimated angles by the proposed algorithm at 1000rpm and 1500rpm, respectively. The experimental results shown at the Figure 11 indicate the dynamic characteristic of the speed, estimated angle, current and flux at the initial starting time using the PI speed controller at 1000[rpm] condition. At the speed response characteristic of the Figure 11, the time reached 500[rpm] is about 0.1[sec] in the condition of no load. Also the peak waveform shown at the part of speed response characteristic is the tolerance of rotor position sensing generated by the noise. The current is less decreased after the detection of rotor position via initial pulse and the flux is more increased because of the voltage establishment.

Table 1 Design parameters of experiment motor

Stator/rotor ploe	6/4	Base load[HP]	1.0HP
Stator OD	135mm	Base speed	1280rpm
Stator ID	87.5mm	Airgap	0.32mm
Stator pole-arc	30^0	The number of Winding per phase	100
Rotor pole-arc	45^0	Conductor diameter	1.0mm
Stator pole height	13.7mm	Min. inductance	7.9mH
Rotor pole height	12.4mm	Max. inductance	65.2mH

The Figure 12 shows the experimental results of speed response characteristic, then the time reached 500[rpm] is about 0.3[sec] at load condition. The bottom of Figure 12 (a) shows the estimated angle variation. The voltage variation is happened by the variable voltage source which is controlled via chopper in the input stage. Then the current is constant and the flux is changed due to the variable voltage for the speed changing.

The Figure 13(a) shows the speed response characteristic results of PI controller for a loaded condition at steady state. At the speed control using PI controller, as having disturbance the speed is decreased about 200[rpm], and after 2 second, we can see the speed is to reach at steady state. Then, the estimated angle is continuously generated in accordance with real time calculation of rotor angle via voltage increasing and the flux variation. At the Figure 13(b), the flux is increased from 120[mWb] to 140[mWb] after having the disturbance.

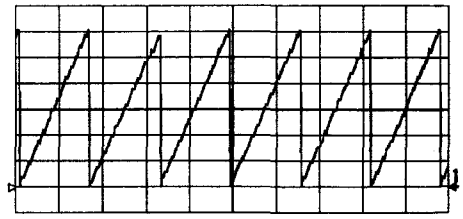

[x axis : 2ms/div, y axis : 500mV/div]
(a) The real angle

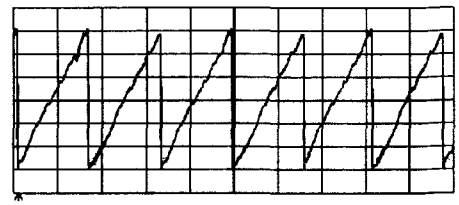

[x axis : 2ms/div, y axis : 500mV/div]
(b) The estimated angle

Fig. 9 The comparison of the real and estimated angle (θ_{on} = 0° , θ_{off} =25° , 1000rpm)

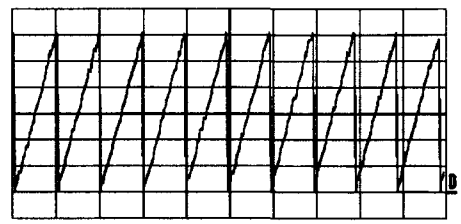

[x axis : 2ms/div, y axis : 500mV/div]
(a) The real angle

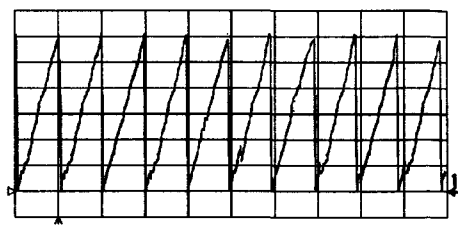

[x axis : 2ms/div, y axis : 500mV/div]
(b) The estimated angle

Fig. 10 The comparison of the real and estimated angle (θ_{on} = 0° , θ_{off} =25° , 1500rpm)

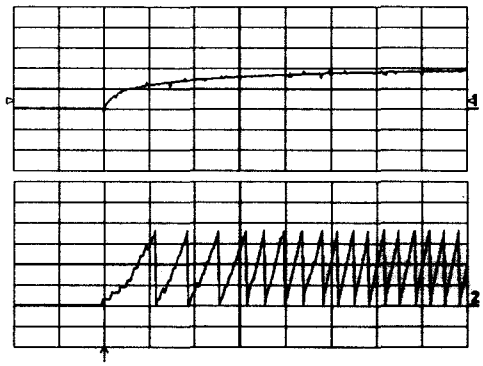

[1 : 500rpm/div, 0.2s/div], [2 : 100deg/div, 0.2s/div]

(a) Initial speed and estimated angle at 1000[rpm]

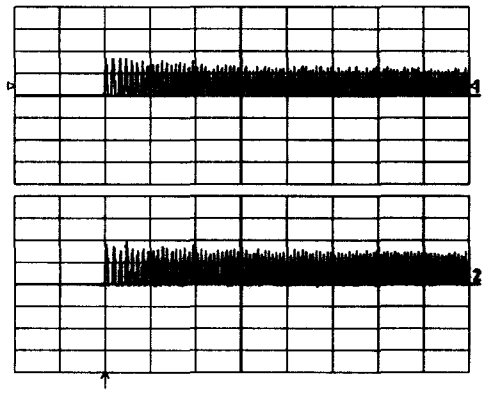

[1 : 1A/div, 0.2s/div], [2 : 50mWb/div, 0.2s/div]

(b) Current and flux linkage for phase A at 1000[rpm]

Fig. 11 Initial speed, estimated angle, current and flux linkage using PI control at no load and 1000[rpm] condition. (θ_{on} = 0° , θ_{off} =25° , 1000rpm)

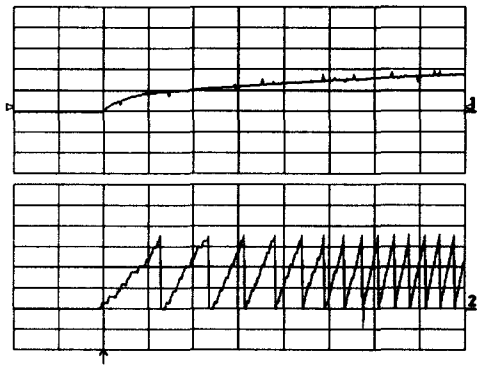

[1 : 500rpm/div, 0.2s/div], [2 : 100deg/div, 0.2s/div]

(a) Speed response characteristic and estimated angle

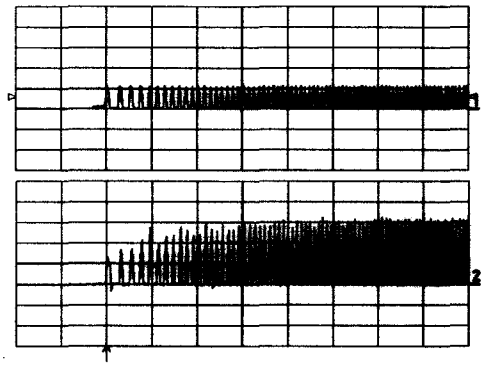

[1 : 1A/div, 0.2s/div] [2 : 50mWb/div, 0.2s/div]

(b) Current and flux linkage of phase A for speed Variation

Fig. 12 Initial speed response, estimated angle, current and flux linkage using PI control at load condition at 1000[rpm].

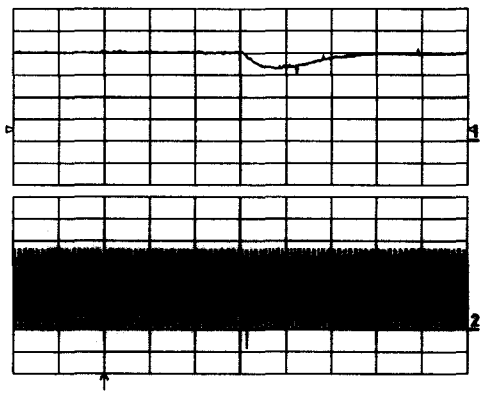

[1 : 250rpm/div, 1s/div] [2 : 100deg/div, 1s/div]

(a) Speed response characteristic and estimated angle for load variation

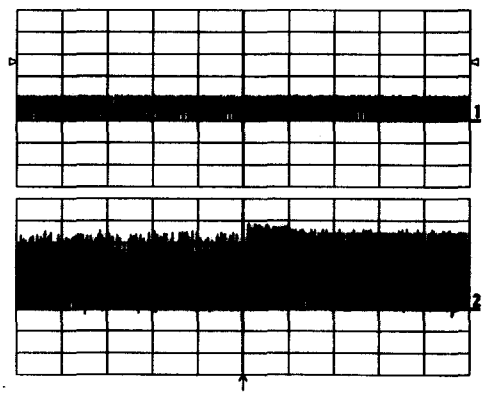

[1 : 1A/div, 1s/div] [2 : 50mWb/div, 1s/div]

(b) Current and flux linkage of phase A for load variation

Fig. 13 Speed response characteristic of PI controller for the rated load injection at 1000[rpm].

5. Conclusion

The magnetizing characteristics estimated from the phase voltage and phase current is described to predict rotor position of SRM. The sensorless control algorithm using neural network is proposed and analyzed.

The optimal phase selector to get continuous rotor position is designed and the error angle analysis result is given at appointed sampling frequency. The performance of proposed rotor position estimation algorithm is verified via the experimental results at variable speed.

참 고 문 헌

[1] P.P. Acarnley, R.J. Hill, and C.W. Hooper, "Detection of rotor position in stepping and switched reluctance motor by monitoring of current waveforms", IEEE Transaction IE, Vol. 32, pp. 215-222, 1985.

[2] J.P.Lyons, S.R.MacMinn, and M.A.Preston, "Flux/ current methods for srm rotor position estimation", Proc. IEEE IAS'91, pp. 482-487, 1991.

[3] J.D. Choi et al., "A Study of SRM sensorless Control using Neural Network", International Power Electronics Conference, Vol.3, pp1160-1165, 2000.

[4] S.R. MacMinn, W.J. Rzesos, P.M. Szczensny, and T.M. Jahns, "Application of sensor integration techniques to switched reluctance motor drives", Proc. IEEE IAS'88, pp. 584-588, 1988

[5] M. Ehsani, I. Husain, and A.B. Kulkarni, "Elimination of discrete position sensor and current sensor in switched reluctance motor drives", IEEE Transaction IA, Vol 28, pp. 128-135, 1992.

[6] P.C. Kjaer, F. Blaajerg, J.K. Pedersen, P. Nielsen, and L. Andersen, "A new indirect rotor position sensor and current sensor in switched reluctance motor drives", Proc. ICEM'94, pp. 555-560, 1994.

[7] G. Gallegos-Lopez, P.C Kjaer, and T.J. E. Miller, "A new sensorless method for switched reluctance motor drives", Proc. IEEE IAS'97, pp. 564-570, 1997.

[8] N. Ertugal and P.P. Acarnley, "A new algorithm for sensorless operation of permanent magnet motors", IEEE Transaction IA, Vol. 30, pp. 126-133, 1994.

저 자 소 개

최 재 동 (崔 載 東)

1967년 11월 25일 생. 1993년 충남대학교 전기공학과 졸업. 1995년 동 대학원 졸업(석사). 2000년 동 대학원 졸업(공박). 1995년~1996년 한국과학기술원 인공위성 연구센터 연구원. 현재 한국항공우주연구원 선임연구원

Tel : 042-860-2498, Fax : 042-860-2007
E-mail : jdchoi@kari.re.kr

안 재 황 (安 載 晃)

1968년 4월 10일 생. 1990년 충남대학교 전기 공학교육학과 졸업. 1993년 동 대학원 전기공학과 졸업(석사). 1999년 동 대학원 박사과정 수료. 현재 동호공고 전기과 교사

Tel : 02-2281-3259, Fax : 02-2281-0095
E-mail : jhahn@dongho-th.ed.seoul.kr

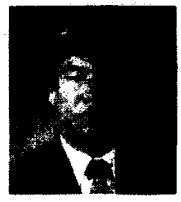

성 세 진 (成 世 鎭)

1948년 7월 15일 생. 1973년 서울대공대 공업교육과 졸업. 1975년 동 대학원 졸업(석사). 1988년 일본 동경공업대 대학원 졸업(공박). 현재 충남대 공대 정보통신공학부 교수. 전력전자학회 회장

Tel : 042-821-7603, Fax : 042-823-3178
E-mail : sjseong@cnu.ac.kr